

The electronic structure of $\text{LiFe}_{15/16}\text{Mg}_{1/16}\text{PO}_4$: *Ab initio* approach

Hong-Lae Park, Sung-Chul Yi^a and Yong-Chae Chung*

Department of Materials Science and Engineering, Hanyang University, Seoul 133-791, Korea

^aDepartment of Chemical Engineering, Hanyang University, Seoul 133-791, Korea

Using the density functional theory based projector-augmented wave method, the electronic structure and electron conducting properties were quantitatively investigated for LiFePO_4 and $\text{LiFe}_{15/16}\text{Mg}_{1/16}\text{PO}_4$. Doping by the Mg atoms into the Fe sites of the LiFePO_4 turned out to enhance the electron localization at the Fe sites, and consequently, the frequency of small polaron hopping was increased, while the band gap remained unchanged. Additionally, the energy barrier for diffusion of Li ions was calculated to be 0.279 eV and the corresponding diffusion coefficient was $4.5 \times 10^{-9} \text{ cm}^2/\text{s}$ for $\text{LiFe}_{15/16}\text{Mg}_{1/16}\text{PO}_4$.

Key words: LiFePO_4 , $\text{LiFe}_{15/16}\text{Mg}_{1/16}\text{PO}_4$, first-principle calculations, electronic structure, electronic conductivity, cathode material, lithium ion battery.

Introduction

The performance of lithium ion batteries for application in portable electronic devices is generally known to be largely affected by atomistic behavior and the electronic structure of cathode materials [1-3]. Due to the non-toxicity, abundance, high specific capacity, and excellent capacity retention, LiFePO_4 is a promising candidate as a new cathode material in rechargeable lithium batteries. However, the extremely low electronic conductivity of $\sim 10^{-9} \Omega^{-1}\text{cm}^{-1}$ at room temperature is considered to be a major barrier which need to be overcome for an application as a cathode material [4, 5].

Bewlay et al. reported an increment of conductivity, up to seven orders of magnitude by adding a carbon source into LiFePO_4 raw materials [6]. It was also reported that solid-solution doping with a metallic element with supervalency such as Nb^{5+} , Ti^{4+} , Zr^{4+} , Al^{3+} and Mg^{2+} at Li sites significantly increased the electronic conductivity by a factor of $\sim 10^8$ [7]. Another related study demonstrated that the doping with higher valency or bivalent cations could increase the electronic conductivity of cathode materials. [8] Recently, Wang et al. found, experimentally, that the Li battery system with LiFePO_4 doped with a bivalent cation at Fe-sites showed considerably improved performance [9]. And the improvement of the corresponding performance by Fe-site doping could be reasonably explained by the electronic conductivity enhancement (from $\sim 10^{-9} \Omega^{-1}\text{cm}^{-1}$ to $\sim 10^{-7} \Omega^{-1}\text{cm}^{-1}$).

These previous studies give rough an approximate picture of the relation between the alien element doping and the increment of conductivity. However, the atomistic behavior and electronic structure of the LiFePO_4 system together with the doping process still need to be quantitatively investigated for further improvement. In this study, using a projector-augmented wave method based on a density functional theory, structural properties including the lattice parameters and displacement of constituent atoms, and the electronic densities of states and different charge densities were quantitatively analyzed. Also, the activation energy barrier for Li^+ ion diffusion and corresponding diffusion coefficient, D were calculated.

Calculation Methods

Using the Vienna *ab initio* simulation program (VASP), [12] a *ab initio* density functional calculation was performed in a projector augmented wave (PAW) method [10] with the generalized gradient approximation (GGA+U) [11]. The GGA+U was chosen to remove the false self-interaction in the calculation step for transition metal oxides in GGA [13]. An U-J value of 4.3 eV in the GGA+U scheme was chosen for the extended super cell of 112 atoms of 4 orthombic LiFePO_4 units. A plane wave basis was expanded up to the energy cut off of 500 eV and k-points in the Brillouin zone were set to follow $4 \times 4 \times 4$ Gamma Monkhorst pack grids. All the atomic positions, the lattice parameters, and the cell volume were fully relaxed until the remaining interatomic forces became in the range of 0.01 eV/Å.

The Li ion diffusion constant can be calculated from the activation energy barrier for the diffusion of a Li ion from one occupied site to an adjacent vacant site.

*Corresponding author:
Tel : +82-2-2220-0507
Fax: +82-2-2281-5308
E-mail: yongchae@hanyang.ac.kr

Diffusion of Li ions through one-dimensional channels was considered in the 4 formula units with 15 Li ions and 1 Li vacant site. The total energy was calculated from the potential energy map corresponding to the movement of a Li atom from the lattice site to the adjacent vacant site. [15, 16] The diffusion constant is well known to take the simple relation $D = \Gamma\alpha^2$, where Γ is the hopping frequency between two adjacent sites and α is the corresponding interatomic distance. The hopping frequency Γ is represented by the relation of $\Gamma \approx \nu_0 \exp(-E_{\text{act}}/k_B T)$, where ν_0 is the attempt frequency and E_{act} is the activation energy barrier [17].

Result and Discussion

Figure 1 shows the crystalline structure of LiFePO_4 in the $1 \times 2 \times 2$ extended super cell. One formula cell is composed of four sets of three cation-centered polyhedrons; a PO_4 tetrahedron, a FeO_6 octahedron, and a LiO_6 octahedron. The oxygen ions of the FeO_6 octahedron formed a layer of edge-sharing through the b - c plane. In this structure, the electron could be transferred along one layer but not through the interlayer, since each layer is separated by a PO_4 tetrahedron layer. The calculated theoretical lattice parameters and atomic positions of LiFePO_4 are summarized and compared with the experimental values in Table 1 [18]. All of the calculated lattice parameters are within the range of 1% compared to the experimental data and the calculated atomic positions are also in excellent agreement with the experimental observations, which can reasonably represent the accuracy of our calculations. The calculated values of $\text{LiFe}_{15/16}\text{Mg}_{1/16}\text{PO}_4$ are also listed in Table 1. It can be clearly seen that the lattice parameters of Mg-doped LiFePO_4 and pure LiFePO_4 are very similar.

Since the charge/discharge cycle of a Li ion battery is mainly dominated by Li ion diffusion and electron transfer through the cathode material, both electronic and ionic conduction should be considered to maintain the charge neutrality during Li ion cycling. For the case of electronic conduction two feasible conducting

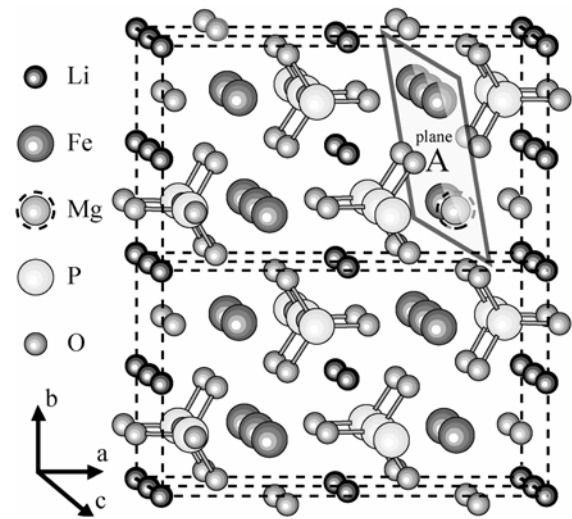


Fig. 1. Crystal Structure of The LiFePO_4 system formed from $1 \times 2 \times 2$ super cells.

mechanisms could be considered: conventional electron conduction by the excitation of the electron through the narrow band gap, and a small polaron hopping process of electron. The spin-polarized density of states of LiFePO_4 and $\text{LiFe}_{15/16}\text{Mg}_{1/16}\text{PO}_4$ using the GGA+U scheme was calculated and shown in Fig. 2, from which the magnitude of the bandgap could be quantitatively obtained. The LiFePO_4 turned out to be a semiconductor with a large band gap 3.317 eV and $\text{LiFe}_{15/16}\text{Mg}_{1/16}\text{PO}_4$ had a slightly smaller band gap of 3.305 eV compared to pure LiFePO_4 . It can be reasonably concluded that the bandgap conduction could not be a major mechanism, and also the doping with Mg cannot significantly change the value of the bandgap energy.

In an attempt to obtain a clear picture of the electron behavior, the difference in electron density between LiFePO_4 and FePO_4 planes with a maximum number of Fe atoms was calculated to observe the electron transfer between Fe sites during the Li intercalation process (Fig. 3). The electron density of the FePO_4 system was obtained using the lattice parameters and

Table 1. Experimental and calculated structural parameters of LiFePO_4 and $\text{LiFe}_{15/16}\text{Mg}_{1/16}\text{PO}_4$

	LiFePO_4 (Exp)			LiFePO_4 (Cal)			$\text{LiFe}_{15/16}\text{Mg}_{1/16}\text{PO}_4$ (Cal)		
	a (Å)	b (Å)	c (Å)	a (Å)	b (Å)	c (Å)	a (Å)	b (Å)	c (Å)
	10.320	6.007	4.691	10.429	6.074	4.755	10.422	6.061	4.754
	x	y	z	x	y	z	x	y	z
Li	0	0	0	0	0	0	0	0	0
Fe	0.282	1/4	0.972	0.281	1/4	0.976	0.281	1/4	0.976
P	0.095	1/4	0.418	0.095	1/4	0.420	0.095	1/4	0.420
O ₁	0.095	1/4	0.740	0.096	1/4	0.744	0.096	1/4	0.744
O ₂	0.454	1/4	0.206	0.457	1/4	0.206	0.457	1/4	0.207
O ₃	0.162	0.052	0.286	0.166	0.046	0.287	0.164	0.047	0.287

Atomic coordinates x, y, and z are given in units of a, b, and c.

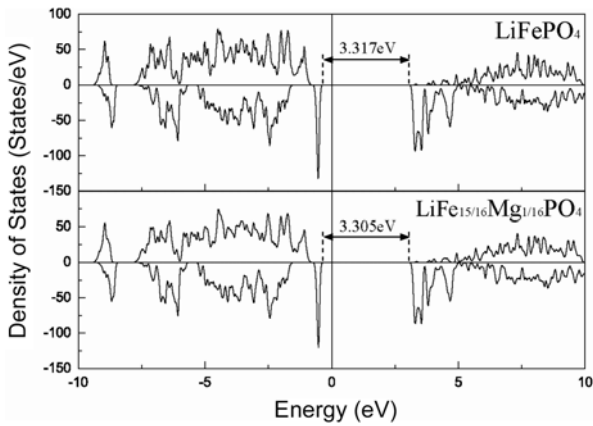


Fig. 2. Density of States of LiFePO_4 and $\text{LiFe}_{15/16}\text{Mg}_{1/16}\text{PO}_4$ near the Fermi level.

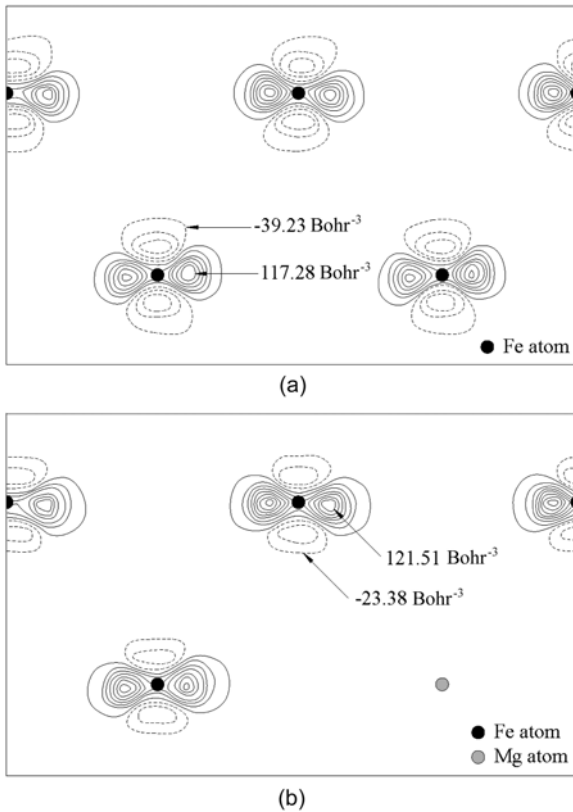


Fig. 3. Difference charge density contour plot for Li intercalation in (a) LiFePO_4 , and (b) $\text{LiFe}_{15/16}\text{Mg}_{1/16}\text{PO}_4$. The planes illustrated correspond to the plane A of Fig. 1. An accumulated region and a depletion region of charge density are demonstrated by solid and dotted lines, respectively. The contour lines are separated by a spacing of 17.39 Bohr^{-3} for (a), and 16.10 Bohr^{-3} for (b).

atomic coordination of the LiFePO_4 system in order to normalize the difference of electron density. The calculated contour plots of the different densities showed significant change of electron density near Fe atoms during the Li intercalation process. The electrons accumulated around Fe sites by the Li intercalation, which is accompanied by the transformation of Fe atoms from the $\text{Fe}^{3+}(t_{2g}^3 e_g^2)$ into the $\text{Fe}^{2+}(t_{2g}^4 e_g^2)$. It

Table 2. Calculated activation barriers and diffusion constants for Li diffusion

Material	E_{act} (meV)	D (cm^2/s)*
LiFePO_4	290.1	3.1×10^{-9}
$\text{LiFe}_{15/16}\text{Mg}_{1/16}\text{PO}_4$	279.0	4.5×10^{-9}

* D is calculated using $D = \alpha^2 \nu_0 \exp(-E_{\text{act}}/k_B T)$ with $\nu_0 = 10^{12} \text{ Hz}$ (s^{-1}), $k_B = 1.380622 \times 10^{-16} \text{ erg/K}$

could be reasonably assumed that LiFePO_4 containing mixed-valent $\text{Fe}^{2+}/\text{Fe}^{3+}$ may exhibit electron transport associated with small polaron hopping as in other transition metal oxides [19, 20]. Moreover, it can be seen that the electron accumulation increased and the electron depletion at Fe sites decreased by Mg doping: from $(-39.23 \sim 117.28) \text{ Bohr}^{-3}$ to $(-23.38 \sim 121.51) \text{ Bohr}^{-3}$. This means that the Mg doping could enhance the electron concentration near Fe sites. Consequently, the degree of electron transport by small polaron hopping could be increased by Mg doping.

Additionally, the activation barriers and Li diffusion constants for pure LiFePO_4 and $\text{LiFe}_{15/16}\text{Mg}_{1/16}\text{PO}_4$ were calculated and are listed in Table 2. The diffusion constants D were obtained from the calculated activation energy barriers with a the hopping distance of 3 \AA , with the phonon frequency assumed to be $\nu_0 = 10^{12} \text{ Hz}$, and Boltzmann constant $k_B = 1.380622 \times 10^{-23} \text{ J/K}$. The activation energy barrier of 290.1 eV for $\text{LiFe}_{15/16}\text{Mg}_{1/16}\text{PO}_4$ was noticeably smaller than the corresponding value for LiFePO_4 of 279.0 eV . Consequently, the diffusion constant was increased to $4.5 \times 10^{-9} \text{ cm}^2/\text{s}$ for $\text{LiFe}_{15/16}\text{Mg}_{1/16}\text{PO}_4$ from $3.1 \times 10^{-9} \text{ cm}^2/\text{s}$ for LiFePO_4 , which could clearly demonstrated that the Mg doping enhanced the Li ion diffusion in the LiFePO_4 system. It is worth mentioning that the estimated diffusion constants of the LiFePO_4 system in this study is in the range of the same order of magnitude that has been experimentally found for LiCoO_2 of $10^{-13} \sim 10^{-7} \text{ cm}^2/\text{s}$ [21].

Conclusions

An *ab-initio* calculation was performed to investigate the electronic structure and electron conducting properties of LiFePO_4 and $\text{LiFe}_{15/16}\text{Mg}_{1/16}\text{PO}_4$. The calculated bandgap energy of $\text{LiFe}_{15/16}\text{Mg}_{1/16}\text{PO}_4$ was slightly decreased to 3.305 eV compared to 3.317 eV for pure LiFePO_4 . Thus, the bandgap conduction through such a large bandgap could not be a major transport mechanism and also the doping with Mg cannot significantly change the degree of electronic conduction via the badngap. A charge density calculation showed the locally accumulated electrons near the Fe sites during the Li intercalation process, which resulted in the formation of mixed-valent $\text{Fe}^{2+}/\text{Fe}^{3+}$, could be indirect evidence for a small polaron hopping mechanism. Moreover, it can be seen that, by Mg doping, the

electron accumulation near Fe sites increased and by contrast the electron depletion was decreased. Consequently, it can be reasonably concluded that Mg doping at Fe sites could increase the electron transport by the small polaron hopping in LiFePO₄ system which could result in an increment of electronic conductivity.

References

1. G. Ceder, Y.-M. Chiang, D.R. Sadoway, M.K. Aydin, Y.-I. Jang, and B. Huang, *Nature* 394 (1998) 694-696.
2. J. Kim and A. Manthiram, *Nature* 390 (1997) 265-267.
3. J.-M. Tarascon and M. Armand, *Nature* 414 (2001) 359-367.
4. A. Yamada, S. Chung, and K. Hinojuma, *J. Electrochem. Soc.* 148 (2001) A224-A229.
5. J.F. Ni, H.H. Zhou, J.T. Chen, and X.X. Zhang, *Mater. Lett.* 59 (2005) 2361-2365.
6. S.L. Bewlay, K. Konstantinov, G.X. Wang, S.X. Dou, and H.K. Liu, *Mater. Lett.* 58 (2004) 1788-1791.
7. S.Y. Chung, J.T. Bloking, and Y.-M. Chiang, *Nat. Mater.* 1 (2002) 123-128.
8. S.Q. Shi, L. Liu, C.O. Ouyang, D.S. Wnag, Z.X. Wnag, L. Chen, and X. Huang, *Phys. Rev. B* 68 (2003) 195108-1-5.
9. D. Wang, H. Li, S.Q. Shi, X.J. Huang, and L.Q. Chen, *Electrochim. Acta* 50 (2005) 2955-2958.
10. P.R. Blochl, *Phys. Rev. B* 50 (1994) 17953-17979.
11. G. Kresse and J. Hafner, *Phys. Rev. B* 47 (1993) 558-561.
12. J.P. Perdew, J.A. Chevary, S.H. Vosko, K.A. Jakson, M.R. Pederson, D.J. Singh, and C. Fiolhais, *Phys. Rev. B* 46 (1992) 6671-6687.
13. C.A. Marianetti, M. Cococcioni, D. Morgan, and G. Ceder, *Phys. Rev. B* 69 (2004) 201101-1-4.
14. F. Zhou, K. Kang, T. Maxisch, G. Ceder, and D. Morgan, *Solid State Comm.* 132 (2004) 181-186.
15. C.Y. Ouyang, S.Q. Shi, Z.X. Wang, H. Li, X.J. Huang, and L.Q. Chen, *J. Phys.: Condens. Matter* 16 (2004) 2265-2272.
16. C.Y. Ouyang, S.Q. Shi, Z.X. Wang, X.J. Huang, and L.Q. Chen, *Phys. Rev. B* 69 (2004) 104303-1-5.
17. D. Morgan, A. Van der Ven, and G. Ceder, *Electrochem. Solid-State Lett.* 7 (2004) A30-A32.
18. A.S. Andersson, B. Kalska, L. Häggström, and J.O. Thomas, *Solid State Ionics* 130 (2000) 41-52.
19. B. Ammundsen and J. Paulsen, *Adv. Mater.* 13 (2001) 943-956.
20. M.S. Islam, R.A. Davies, and J.D. Gale, *Chem. Mater.* 15 (2003) 4280-4286.
21. Y.-I. Jang, B.J. Neudecker, and N.J. Dudney, *Electrochem. Solid-State Lett.* 4 (2001) A74-A77.